Journal of Inorganic Biochemistry xxx (2015) xxx–xxx

Contents lists available at ScienceDirect

Journal of Inorganic Biochemistry

journal homepage: www.elsevier.com/locate/jinorgbio

Vanadium(IV) and copper(II) complexes of salicylaldimines and aromatic heterocycles: Cytotoxicity, DNA binding and DNA cleavage properties

Isabel Correia [a,*], Somnath Roy [a], Cristina P. Matos [a], Sladjana Borovic [a,b], Nataliya Butenko [a,b], Isabel Cavaco [a,b], Fernanda Marques [c], Julia Lorenzo [d], Alejandra Rodríguez [e], Virtudes Moreno [e], João Costa Pessoa [a,*]

[a] Centro de Química Estrutural, Instituto Superior Técnico, Universidade de Lisboa, Av. Rovisco Pais, 1049-001 Lisboa, Portugal
[b] Departamento de Química, Bioquímica e Farmácia, Faculdade de Ciências e Tecnologia, Universidade do Algarve, Campus de Gambelas, 8005-139 Faro, Portugal
[c] Centro de Ciências e Tecnologias Nucleares, Instituto Superior Técnico, Universidade de Lisboa, Estrada Nacional 10 (km 139.7) 2695-066 Bobadela LRS, Portugal
[d] Institut de Biotecnologia i Biomedicina, Universidad Autonoma Barcelona, Bellaterra, 08193 Barcelona, Spain
[e] Departamento de Química Inorgánica, Universitat Barcelona, Martí i Franquès 1-11, 08028 Barcelona, Spain

ARTICLE INFO

Article history:
Received 24 November 2014
Received in revised form 26 February 2015
Accepted 27 February 2015
Available online xxxx

Keywords:
Copper(II)
Vanadium(IV)
Salicylaldimines
Heterocycles
Metallonucleases

ABSTRACT

Five copper(II) complexes, [Cu(sal-Gly)(bipy)](**1**), [Cu(sal-Gly)(phen)] (**2**), [Cu(sal-L-Ala)(phen)] (**3**), [Cu(sal-D-Ala)(phen)] (**4**), [Cu(sal-L-Phe)(phen)] (**5**) and five oxidovanadium(IV) complexes, [V^{IV}O(sal-Gly)(bipy)] (**6**), [V^{IV}O(sal-Gly)(phen)] (**7**), [V^{IV}O(sal-L-Phe)(H_2O)] (**8**), [V^{IV}O(sal-L-Phe)(bipy)] (**9**), [V^{IV}O(sal-L-Phe)(phen)] (**10**) (sal = salicylaldehyde, bipy = 2,2′-bipyridine, phen = 1,10-phenanthroline) were synthesized and characterized, and their interaction with DNA was evaluated by different techniques: gel electrophoresis, fluorescence, UV–visible and circular dichroism spectroscopy. The complexes interact with calf-thymus DNA and efficiently cleave plasmid DNA in the absence (only **2** and **5**) and/or presence of additives. The cleavage ability is concentration-dependent as well as metal and ligand-dependent. Moreover, DNA binding experiments show that the phen-containing Cu^{II} and $V^{IV}O$ compounds display stronger DNA interaction ability than the corresponding bipy analogues. The complexes present cytotoxic activity against human ovarian (A2780) and breast (MCF7) carcinoma cells. Cell-growth inhibition (IC_{50}) of compounds **1**, **2** and **5** in human promyelocytic leukemia (HL60) and human cervical cancer (HeLa) cells were also determined. The copper complexes show much higher cytotoxic activity than the corresponding vanadium complexes and the reference drug cisplatin (except for the sal-Gly complexes); namely, the phenanthroline copper complexes **2**–**5** are ca. 10-fold more cytotoxic than cisplatin and more cytotoxic than their bipyridine analogues.

1. Introduction

The exploration of transition metal compounds as therapeutics is a challenging and promising area of biochemical research. The last decades have seen an exponential growth in metal complexes being developed as new drugs for challenging diseases, such as parasitic-related infections, since despite current advancements, progress in this area has been rather slow [1–3].

An important step in drug design is identifying the drug target. For cancer, DNA has been pointed as one of the targets and, thus, the DNA binding and cleavage activity by redox active metal complexes is a key information when developing efficient anticancer drugs. DNA can be cleaved by hydrolytic or oxidative mechanisms, with the oxidative route being the most common for redox-active metal complexes. This has led to a considerable increase in the search for metallonucleases as anticancer therapeutics [4–11].

The interest in the medicinal applications of vanadium complexes [12] is largely due to its insulin-enhancing properties [13–16], its potential antitumor [17–20], its antiparasitic action [19–24] and effects on many enzymes [12,25–28]. Over the last decades vanadium compounds have shown positive *in vitro* effects in several animal cancer models, and have shown protection against all stages of carcinogenesis [12,29]. Copper compounds, which normally have lower toxicity than nonessential metal ions like platinum, have been regarded as an anticancer alternative to cisplatin, due to their redox properties [1,30,31]. Their ability to induce hydrolysis or oxidative cleavage of DNA is another positive characteristic, and Cu^{II} complexes are among the most extensively studied chemical nucleases [6,32,33]. Usually, the DNA cleavage activity of Cu^{II} complexes is observed in the presence of oxidizing or reducing co-reactants. However, a few copper complexes were reported to have a remarkable capability to cleave DNA, not requiring the presence of oxidizing or reducing agents [9,11,34,35].

Oxidovanadium(IV/V) and copper(II) complexes with salicylaldimine ligands derived from amino acids and aldehydes have been a focus of interest for several decades [36–45]. $V^{IV}O$ and Cu^{II} ternary complexes of the type M(sal-AA)(NN) where sal-AA is a Schiff base

* Corresponding authors. Fax: +351 218419239.
E-mail addresses: icorreia@tecnico.ulisboa.pt (I. Correia), joao.pessoa@tecnico.ulisboa.pt (J.C. Pessoa).

http://dx.doi.org/10.1016/j.jinorgbio.2015.02.021
0162-0134/

derived from the condensation of α-amino acids with salicylaldehyde and NN are planar N-donor heterocyclic bases, have also been known for many years [39,41,42,44], but have recently attracted a renewed interest [46–50]. The reason is the heterocyclic base that renders the complex able to bind DNA through intercalation or surface and/or groove binding [49]. Additionally, the Schiff base, containing different amino acids, may be synthesized with varied structures, can participate in acid/base equilibria through their potentially labile carboxylate and/or side groups, and the metal ions under physiological conditions are redox active and can induce the production of ROS, DNA being oxidatively cleaved.

In the present work, five ternary Cu^{II}-complexes and five $V^{IV}O$-complexes, of the type [M(sal-AA)(NN)], were synthesized and characterized by elemental analysis, UV–visible (UV–vis), and IR spectra. The DNA binding ability of the complexes was evaluated by interaction studies with calf-thymus DNA (CT-DNA) using UV–vis absorption, fluorescence, circular dichroism (CD) and atomic force microscopy (AFM). Their DNA cleavage ability was evaluated by gel electrophoresis with plasmid DNA. In addition, the cytotoxicity of the complexes against the human ovarian carcinoma cells (A2780) and breast adenocarcinoma cells (MCF 7) was assessed by the MTT ([3-(4,5-dimethylthiazol-2-yl)-2,5-diphenyltetrazolium bromide]) assay. Cell-growth inhibition in HeLa and HL60 cell lines was also determined for some of the Cu^{II}-complexes.

2. Methods

2.1. General procedures

$V^{IV}OSO_4$, $Cu^{II}(acac)_2$ (acac = acetylacetone), 1,10-phenanthroline and 2,2′-dipyridyl were purchased from Sigma Aldrich. Other materials were obtained from commercial sources and used as received. Phosphate buffered saline (PBS) from Sigma-Aldrich was used for the preparation of solutions for spectroscopic DNA experiments. The composition of one tablet dissolved in 200 ml of Millipore water yields 0.010 M phosphate buffer, 0.0027 M potassium chloride and 0.137 M sodium chloride, pH 7.4, at 25 °C. Millipore® water was used for the preparation of all solutions and produced using a Millipore Milli-Q® Academic water purification system. Absolute ethanol (EtOH, Panreac Química, S.A.) was used for the preparation of stock solutions of complexes and for the solution used in all spectroscopic experiments with these compounds, i.e. the solution containing 95% of PBS buffer and 5% EtOH. Unless otherwise stated, reagents were commercially available and of analytical grade.

2.2. Physical measurements

Most UV–vis absorption spectra were recorded on a Perkin-Elmer Lambda 35 spectrophotometer equipped with a Peltier temperature-controller at 25 °C. Infrared spectra (IR, 4000–400 cm^{-1}) were recorded either on a Nicolet Impact 400D or on a BIO-RAD FTS 3000 MX spectrophotometer in KBr pellets; wavenumbers are in cm^{-1}. The CD spectra were recorded at 25 °C on a Jasco J-720 spectropolarimeter with UV–vis (200–700 nm) or red-sensitive (400–1000 nm) photomultipliers (EXEL-308). Unless otherwise stated, for isotropic absorption spectra in the 200–400 nm range or 400–1000 nm range we use the abbreviations UV or vis spectra, respectively. Fluorescence spectra were measured on Horiba Jobin Yvon fluorescence spectrometer model FL 1065 at room temperature. ^{51}V-NMR spectra were recorded on a Bruker Avance III 400 MHz instrument.

2.3. Syntheses of the Cu^{II}-complexes

The Cu^{II}-complexes were prepared according to a previously reported procedure [48]. In general, to an aqueous solution of the amino-acid an equimolar solution of salicylaldehyde in methanol was added. The resulting mixture was stirred and heated at about ~60 °C. A few minutes later a methanolic solution of the heterocyclic base (equimolar) and crystalline cupric acetate (equimolar) in water were added.

[Cu(sal-Gly)(bipy)] (1) A greenish solid was obtained. Yield ~77%. Anal. Calcd for $C_{19}H_{15}N_3O_3Cu$ ($3.7H_2O$) Found (Calcd) (%): C 49.14 (49.24); H 4.8 (4.87); N 9.0 (9.07). IR (KBr pellet, cm^{-1}): $\nu_{asym}(CO_2)$ 1654, ν(C = N) 1598, $\nu_{sym}(CO_2)$ 1383 [43]. UV–vis (PBS with 5% EtOH): λ_{max} (nm): 260, 360, 675.

[Cu(sal-Gly)(phen)] (2) A greenish solid was obtained. Yield ~82%. Anal. Calcd for $C_{21}H_{15}N_3O_3Cu$ ($5.5H_2O$) Found (Calcd) (%): C 48.4 (48.51); H 5.1 (5.04); N 7.9 (8.08). IR (KBr pellet, cm^{-1}): $\nu_{asym}(CO_2)$ 1630, ν(C = N) 1601, $\nu_{sym}(CO_2)$ 1372 [43]. UV–vis (PBS with 5% EtOH): λ_{max} (nm): 270, 370, 672.

[Cu(sal-L-Ala)(phen)] (3) A greenish solid was obtained. Yield ~76%. Anal. Calcd for $C_{22}H_{17}N_3O_3Cu$ ($5.7\ H_2O$) Found (Calcd) (%): C 49.1 (49.16); H 5.0 (5.33); N 7.7 (7.82). IR (KBr pellet, cm^{-1}): $\nu_{asym}(CO_2)$ 1639, ν(C = N) 1599, $\nu_{sym}(CO_2)$ 1382 [43]. UV–vis (PBS with 5% EtOH): λ_{max} (nm): 258, 304, 419.

[Cu(sal-D-Ala)(phen)] (4) A greenish solid was obtained. Yield ~76%. Anal. Calcd for $C_{22}H_{17}N_3O_3Cu$ ($1.5H_2O$) Found (Calcd) (%): C 57.0 (57.20); H 4.0 (4.36); N 9.1 (9.10). IR (KBr pellet, cm^{-1}): $\nu_{asym}(CO_2)$ 1633, ν(C = N) 1600, $\nu_{sym}(CO_2)$ 1375 [43]. UV–vis (5% EtOH and PBS): λ_{max} (nm): 257, 305, 417.

[Cu(sal-L-Phe)(phen)] (5) A greenish solid was obtained. Yield ~80%. Anal. Calcd for $C_{28}H_{21}N_3O_3Cu$ ($0.7H_2O$) Found (Calcd) (%): C 64.1 (64.23); H 4.0 (4.31); N 8.0 (8.02). IR (KBr pellet, cm^{-1}): $\nu_{asym}(CO_2)$ 1645, ν(C = N) 1601, $\nu_{sym}(CO_2)$ 1385 [43]. UV–vis (PBS with 5% EtOH): λ_{max} (nm): 255, 308, 420.

2.4. Synthesis of the $V^{IV}O$-complexes

All vanadium complexes were synthesized according to a previously described procedure [39,42] in water/alcohol mixtures. In general, the amino acid dissolved in water was mixed with an equimolar amount of salicylaldehyde in ethanol. The resulting solution was refluxed for 1 h, followed by addition of equimolar aqueous solution of $V^{IV}OSO_4$. To this mixture the equimolar heterocyclic base in methanol was added.

[VO(sal-Gly)(bipy)] (6) A red solid was obtained. Yield ~78%. Anal. Calcd for $C_{17}H_{13}N_3O_4V$ Found (Calcd) (%): C 56.7 (57.01); H 3.8 (3.78); N 10.5 (10.25). IR (KBr pellet, cm^{-1}): ν(V = O) ~963, 940, $\nu_{asym}(CO_2)$ 1653, ν(C = N) 1603, $\nu_{sym}(CO_2)$ 1384 [43,44]. UV–vis (PBS with 5% EtOH): λ_{max} (nm): 284, 330, 395.

[VO(sal-Gly)(phen)] (7) A deep brown solid was obtained. Yield ~80%. Anal. Calcd for $C_{21}H_{15}N_3O_4V$ ($2.2\ H_2O$, $0.3CH_3OH$) Found (Calcd) (%): C 54.0 (54.03); H 4.2 (4.38); N 8.6 (8.87). IR (KBr pellet, cm^{-1}): ν(V = O) ~950 cm^{-1}, $\nu_{asym}(CO_2)$ 1630, ν(C = N) 1600, $\nu_{sym}(CO_2)$ 1384 [43,44]. UV–vis (PBS with 5% EtOH): λ_{max} (nm): 267, 382, 730.

[VO(sal-L-Phe)(H_2O)] (8) A light-bluish precipitate was obtained. Yield ~65%. Anal. Calcd for $C_{16}H_{14}NO_5V$ Found (Calcd) (%): C 54.4 (54.66); H 4.1 (3.98); N 3.9 (3.98). IR (KBr pellet, cm^{-1}): ν(V = O) ~1008, $\nu_{asym}(CO_2)$ 1627, ν(C = N) 1599, $\nu_{sym}(CO_2)$ 1369, $\nu(H_2O)$ 3026 [43,44]. UV–vis (PBS with 5% EtOH): λ_{max} (nm): 265, 325, 430, 720.

[VO(sal-L-Phe)(bipy)] (9) A red solid was obtained. Yield ~72%. Anal. Calcd for $C_{26}H_{21}N_3O_4V$ ($2H_2O$) Found (Calcd) (%): C 59.0 (59.32); H 4.4 (4.79); N 7.9 (7.98). IR (KBr pellet, cm^{-1}): ν(V = O) ~952, $\nu_{asym}(CO_2)$ 1642 cm^{-1}, ν(C = N) 1618; $\nu_{sym}(CO_2)$ 1376 [43,44]. UV–vis (PBS with 5% EtOH): λ_{max} (nm): 262, 316, 428, 720.

Please cite this article as: I. Correia, et al., Vanadium(IV) and copper(II) complexes of salicylaldimines and aromatic heterocycles: Cytotoxicity, DNA binding and DNA cleavage pr..., J. Inorg. Biochem. (2015), http://dx.doi.org/10.1016/j.jinorgbio.2015.02.021

[VO(sal-L-Phe)(phen)] (10) A deep red solid was obtained. Yield ~69%. Anal. Calcd for $C_{28}H_{21}N_3O_4V$ (2.2 H_2O) Found (Calcd) (%): C 60.4 (60.70); H 4.3 (4.62); N 7.7 (7.58). IR (KBr pellet, cm^{-1}): ν(V = O) ~ 955, $\nu_{asym}(CO_2)$ 1647 cm^{-1}, ν(C = N) 1620; $\nu_{sym}(CO_2)$ 1384 [43,44]. UV–vis (PBS with 5% EtOH): λ_{max} (nm): 260, 300, 428, 720.

2.5. DNA experiments

2.5.1. Binding to DNA

Millipore® water was used for the preparation of solutions and PBS buffer was used in all experiments. The binding experiments of CT-DNA with complexes were done with $r_i = 4$ (ri = molar concentration of CT-DNA base pairs:molar concentration of compound) in the wavelength region 240–540 nm, in PBS, using quartz cuvettes (1, 2 or 10 mm path length) at 25 °C. The absorption ratio of CT-DNA solutions at λ_{max} 260 and 280 nm was 1.9, indicating that CT-DNA was sufficiently free from protein impurities. The concentration of DNA in base pairs was determined by UV–vis absorbance using the molar absorption coefficient at 260 nm (6600 M^{-1} cm^{-1}). The CT-DNA sodium salt was purchased from Sigma and used as received. The stock solutions (~1 mg/ml) were prepared by addition of PBS buffer and gentle stirring at 4 °C for 24–48 h and the solutions were used within 4 days after their preparation. The stock solutions of complexes were prepared by dissolving the complexes in ethanol, dilution in PBS buffer; they were always used within a few hours. The amount of ethanol was kept equal to 5% (v/v) in each experiment. The absorption spectra of mixtures containing the complexes (100 μM) and CT-DNA (400 μM) in PBS buffer containing 5% EtOH were measured by monitoring changes with time. ^{51}V NMR spectra were measured with time (up to 24 h) for a sample containing 600 μM of CT-DNA and 150 μM VO(sal-Gly)(phen) in PBS with 5% EtOH and 5% D_2O. ^{51}V chemical shifts were referenced relative to neat $V^{V}OCl_3$ as the external standard.

The fluorescence titrations were done using a quartz cuvette of 1 cm path length. A fluorescence titration was done in which increasing amounts of a CT-DNA solution were added to a solution containing complex **2** (80 μM in 5% EtOH). The samples were exited at 365 nm (slits = 5 nm) and the emission spectra were recorded between 400 and 650 nm. UV–vis absorption spectra were collected to correct the data for inner filter effects [51,52]. The CT-DNA concentration was varied from 0 to 200 μM and the Stern–Volmer dynamic quenching constant, K_{SV}, was calculated according to the classical Stern–Volmer equation: $I_{F0}/I_F = 1 + K_{SV}[DNA]$, where I_{F0} and I_F are the fluorescence intensities of complex **2** in the absence and in the presence of DNA, respectively and [DNA] is the molar DNA concentration in base pairs. For the Stern–Volmer plot the emission at 502 nm was used.

In the competition fluorescence titrations with ethidium bromide (EB) the DNA–EB samples were excited at 360 nm and the emitted fluorescence was recorded between 400 and 700 nm. Since the complexes show fluorescence, blank fluorescence spectra, used to correct the fluorescence spectra of the samples, were measured in the same range, containing everything except EB. Fluorescence emission intensity was corrected for the absorption and emission inner filter effects [51,52] using the UV–vis absorption data recorded for each sample. Bandwidth was typically 5 nm in both excitation and emission. All experiments were carried out in PBS solution containing a maximum of 5% EtOH. The CT-DNA concentration in the experiments was ca. 10 μM and the concentration of complexes varied from 0 to 40 μM. Previously, the saturation of the fluorescence intensity was monitored by addition of increasing amounts of an EB solution to a DNA solution (10 μM), in the range 1 to 10 μM and fluorescence saturation was observed for a concentration of 10 μM of EB, which was then used in the competition experiments. The Stern–Volmer dynamic quenching constant K_{SV} was calculated according to the classical Stern–Volmer equation: $I_{F0}/I_F = 1 + K_{SV}[C]$, where I_{F0} and I_F are the fluorescence intensities of DNA–EB in the absence and in the presence of the complex, respectively and [C] is the copper complex concentration, ranging from 0 to 40 μM. For the Stern–Volmer plots the emission at 611 nm was used.

2.5.2. DNA cleavage

Plasmid DNA pA1, which consists of a full-length cDNA from cytochrome P450 CYP3A1, was inserted in the PBS plasmid vector (pBluescibe, Stratagene, UK) [53] and used for gel electrophoresis experiments (1% agarose gel in TBE 0.5x). The plasmid DNA was amplified in *Escherichia coli* MACH1 and purified using Nucleobond® AX Anion Exchange Columns for quick purification of nucleic acids from MACHEREY-NAGEL. The concentration of pDNA was measured spectroscopically at λ = 260 nm. Linear DNA controls were obtained by digestion with the single-cutter restriction complex $VO(acac)_2$ and used as reference in agarose gel electrophoresis [7]. DNA cleavage activity was evaluated by monitoring the conversion of supercoiled plasmid DNA (Sc-form I) to nicked circular DNA (Nck-form II) and linear DNA (Lin-form III). Standard deviation for repeatability (s_r) for the peak area within the same gel was estimated as 8%, 6% and 8% for the Sc, Nck and Lin forms, respectively [54].

Each reaction mixture was prepared by adding 8 μl of water, 2 μl (200 ng) of supercoiled DNA, 10 μl of 100/200 μM complex solution in 5% EtOH and 20 mM PBS buffer. The final reaction volume was 20 μl, the final buffer concentration was 10 mM and the final metal concentration varied from 5 to 100 μM. Samples were typically incubated for 1 to 5 h at 37 °C. When indicated, the reaction was carried out in the same buffer but in the presence of oxone (2 mM) or MPA (3-mercaptopropionic acid, 2 mM), EtOH (5%).

After incubation, 5 μl of DNA loading buffer (0.25% bromophenol blue, 0.25% xylene cyanol, 30% glycerol in water, Applichem) were added to each tube and the sample was loaded onto a 1% agarose gel in TBE buffer (89 mM Tris–borate, 1 mM EDTA pH 8.3) containing ethidium bromide (0.5 μg/ml). Controls of non-incubated and of linearized plasmid were loaded on each gel electrophoresis. The electrophoresis was carried out for 3 h at 95–110 V. Bands were visualized under UV light and images captured using an AlphaImagerEP (Alpha Innotech). Peak areas were measured by densitometry using AlphaView Software (Alpha Innotech). Peak areas were used to calculate the percentage (%) of each form (Sc, Nck and Lin), with a correction factor of 1.47 for the Sc form to account for its lower staining capacity by ethidium bromide [55]. The photos chosen for this publication were rearranged to show only the relevant samples. All samples in each figure were obtained in the same run.

2.6. Cell viability assays in human tumor cell lines

The human tumor cell lines HeLa, MCF7 and A2780 were cultured in DMEM containing GlutaMax I (MCF7) and RPMI 1640 (A2780, HL60). All culture media (Gibco, Invitrogen) were supplemented with 10% FBS and 1% penicillin/streptomycin at 37 °C and cells were maintained in a humidified atmosphere of 95% of air and 5% CO_2 (Heraeus, Germany). Cell viability was evaluated using a colorimetric method based on the tetrazolium salt MTT, which is reduced in viable cells to yield purple formazan crystals. Cells were seeded in 96-well plates at a density of 2–5 × 10^4 cells per well in 200 μl of medium and left to incubate overnight for optimal adherence. After careful removal of the medium, 200 μl of a dilution series of the compounds in fresh medium were added and incubation was carried out at 37 °C/5% CO_2 for 24 h. The percentage of DMSO in cell culture medium never exceeded 1%. Cisplatin was first solubilized in saline and then added at the same concentrations as used for the other compounds. At the end of the incubation period the compounds were removed and the cells were incubated with 200 μl of MTT solution (500 μg/ml). After 3–4 h at 37 °C/5% CO_2, the medium was removed and the purple formazan crystals were dissolved in 200 μl of DMSO by shaking. The cell viability was evaluated measuring the absorbance at 570 nm using a plate spectrophotometer

Please cite this article as: I. Correia, et al., Vanadium(IV) and copper(II) complexes of salicylaldimines and aromatic heterocycles: Cytotoxicity, DNA binding and DNA cleavage pr..., J. Inorg. Biochem. (2015), http://dx.doi.org/10.1016/j.jinorgbio.2015.02.021

(Power Wave Xs, Bio-Tek). The cellular viability was calculated dividing the absorbance of each well by that of the control wells (cells with no treatment) and expressed in percentage of control. Each experiment was repeated at least three times and each point was determined in at least six replicates. The IC_{50} values (i.e., compound concentration that induces 50% of cell death) were calculated from plots for cellular viability (%) versus compound concentration with the GraphPad Prism software (version 4.0).

3. Results and discussion

3.1. Syntheses and characterization of complexes

The Cu^{II}- and $V^{IV}O$-complexes were prepared *in situ* using a common synthetic procedure for each set [39,42,48] by reaction of a stoichiometric amount of the corresponding metal salts with the corresponding ligand (and co-ligand); their structural formulae are depicted in Fig. 1. The resulting complexes, **1**–**10**, precipitated as green, bluish and/or red microcrystalline solids, in good yields and were characterized by elemental analysis, UV–vis and FTIR spectroscopies. Most complexes had been previously reported [39,42,48].

In general, the Cu^{II} and the $V^{IV}O$-complexes exhibit comparable spectroscopic features, suggesting that they have similar molecular structures. The characteristic $\nu(V=O)$ band appears as a medium-strong band at ca. 950–1000 cm^{-1} in the FTIR spectra of the $V^{IV}O$-complexes. The $\nu_{asym}(CO_2)$, $\nu(C=N)$ and $\nu_{sym}(CO_2)$ stretches appear at ca. 1640, 1600 and 1380 cm^{-1}, respectively, confirming coordination by the N_{imine} donor and monodentate CO_2^- coordination [43,44,56]. The isotropic electronic absorption spectra of the complexes (see examples included in Supplementary information) depict strong intraligand bands at 230–250 and at 270–300 nm and a more intense band at 375–385 nm, frequently assigned to azomethine π–π* from the Schiff base and week d-d bands. TD-DFT (time-dependent density functional theory) calculations for [$V^{IV}O$(sal-L-Ala)(H_2O)] [44] allowed assignment of these bands to a predominantly LMCT (ligand to metal charge transfer) band ($PhO^- \rightarrow V$), specifically a transition from π* (phenol) to a π V–N bond, also spread over benzene π* and the d_{xz} orbital), thus we favor this assignment for the present set of compounds. Similar assignments were made for e.g. [$V^{IV}O$(sal-L-Met)(phen)] and [$V^{IV}O$(sal-L-Trp)(phen)] [46].

The optically active complexes were also characterized by circular dichroism spectroscopy in methanol. For the two Cu^{II}-complexes derived from alanine (**3** and **4**) roughly symmetric spectra were obtained, as expected. Complex **3**, derived form L-Ala, shows a very broad d-d band with maxima of negative signal centered at ca. 700 nm and a negative band at 375 nm (LMCT $PhO^- \rightarrow V$ band, see above). The spectra of the chiral vanadium complexes **9** and **10**, containing the sal-L-Phe Schiff base, present a weak positive band at ca. 445 nm and two strong negative bands at 370 nm and 285 nm (for **9**, for **10** at 260 nm). The CD spectra of [$V^{IV}O$(sal-amino acidato)(NN)] complexes were previously reported and discussed [41,43,44].

The stability of most complexes in PBS (pH 7.4, containing 5% EtOH) was evaluated by isotropic absorption and circular dichroism spectroscopy. Data (included in supplementary information, Figs. S2–S6) show very high stability for the Cu^{II}-complexes for at least 5 h, since practically no changes are observed in both types of spectra within this time frame, while the $V^{IV}O$ complexes spectra show small changes that are due either to partial oxidation and/or to partial hydrolysis, the order of stability being: [$V^{IV}O$(sal-AA)(phen)] > [$V^{IV}O$(sal-AA)(bipy)] > [$V^{IV}O$(sal-AA)(H_2O)].

3.2. DNA-binding study by UV spectroscopy

Electronic absorption spectroscopy is a simple method to examine the DNA binding mode of metal complexes [57,58]. If the binding involves intercalation, the π* orbital of the intercalated ligand can couple with the π orbital of the DNA base pairs, thus, decreasing the π–π* transition energy and resulting in bathochromism (red shift) and

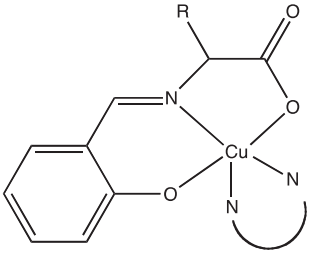

Cu(sal-Gly)(bipy) R = H, NN = bipy (**1**)
Cu(sal-Gly)(phen) R = H, NN = phen (**2**)
Cu(sal-L-Ala)(phen) R = CH_3, NN = phen (**3**)
Cu(sal-D-Ala)(phen) R = CH_3, NN = phen (**4**)
Cu(sal-L-Phe)(phen) R = CH_2-C_6H_5, NN = phen (**5**)

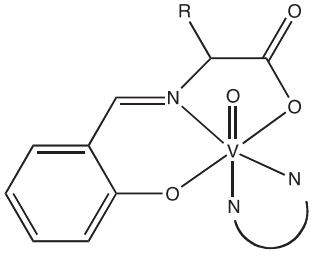

VO(sal-Gly)(bipy) R = H, NN = bipy (**6**)
VO(sal-Gly)(phen) R = H, NN = phen (**7**)
VO(sal-L-Phe)(H_2O) R = CH_2-C_6H_5 (**8**)
VO(sal-L-Phe)(bipy) R = CH_2-C_6H_5, NN = bipy (**9**)
VO(sal-L-Phe)(phen) R = CH_2-C_6H_5, NN = phen (**10**)

NN =

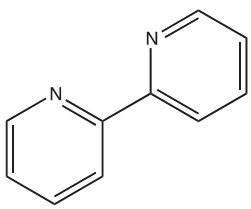

bipy

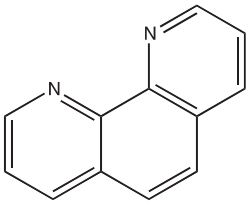

phen

Fig. 1. Structural formula of the Cu^{II} and $V^{IV}O$ complexes and co-ligands.

hypochromism [59,60]. To elucidate the binding ability and type of each complex to DNA, the absorption spectra of solutions containing CT-DNA and the complexes were measured with time for constant CT-DNA (400 μM) and complex (100 μM) concentrations.

Copper complexes containing sal-Gly behave differently depending on the presence of bipy (**1**) or phen (**2**) as co-ligands. For complex **1** addition of DNA to the complex solution results in hypochromism and a red shift in the intraligand band at ca. 270 nm (Fig. S7), however, the changes observed with increasing time, namely the presence of isosbestic points at 244, 290 and 352 nm, and the hyperchromism suggest that the interaction does not involve intercalation [61]. UV absorption spectra measured for CT-DNA in the presence of complex **2** with time are shown in Fig. 2 (for the other complexes see Supplementary Information-SI). In the UV region the intense absorption bands observed in the spectrum of the complex, due to the intraligand π–π* (at 270 nm) and LMCT band (at 365 nm) transitions, decrease in intensity upon mixing with DNA. Additionally, the azomethine band blue shifts its maximum to 355 nm. With time both bands show increased hypochromism. For complexes **3** and **4** (see Figs. S8 and S9) the changes observed were similar. In general, hypochromism has been associated with intercalation as the DNA-binding mode, which has a stabilization effect on the DNA duplex [62]. The complex $[Cu(phen)_2]^{2+}$ was reported to bind by intercalation at the minor groove [63]. It is plausible that the same occurs with complexes **2**–**5**.

Thus, the changes observed in the isotropic absorption spectra immediately upon addition of CT-DNA to the copper complexes **1**–**4** are mainly hypochromism of the LMCT bands and blue shift of the lower energy UV band. This suggests that after mixing with each Cu-complex the interaction with CT-DNA takes place by the direct formation of a complex with double-helical CT-DNA [64]. The hyperchromic effect observed with time after addition CT-DNA to complex **1** might be ascribed to external contact (electrostatic binding) [61], or possibly the complex could uncoil the helix structure of DNA exposing more DNA bases [65]. The similar behavior observed for all phenanthroline containing complexes suggests that it is the heteroaromatic ring that is interacting with the DNA helix, probably by intercalation [61].

As indicated by the UV–vis spectra of e.g. Fig. S4 (and other sets measured), which do not change much with time up to 5 h, complexes $[V^{IV}O(sal\text{-}Gly)(H_2O)]$ and $[V^{IV}O(sal\text{-}Gly)(bipy)]$ are reasonably stable to oxidation and hydrolysis. In contrast, solutions of the same complexes in the presence of CT-DNA depict significant changes (Figs. S10 and S11). Solutions of $[V^{IV}O(sal\text{-}Gly)(H_2O)]$ in the presence of CT-DNA show changes consistent with the formation of a new complex species, probably an adduct between a $V^{IV}O$-complex and DNA (Fig. S10) namely, the disappearance of the bands at 275 and 370 nm, the appearance of new bands at 323 and 257 nm, with isosbestic points at 344, 305 and 264 nm. For $[V^{IV}O(sal\text{-}Gly)(bipy)]$ **6** (Fig. S11), rather similar changes are observed: a decrease in the intensity of bands with maxima at 382 and 280 nm and the appearance of a new band at 326 nm, with isosbestic points at 344 and 318 nm. The spectra obtained after 5 h for the interaction of both $[V^{IV}O(sal\text{-}Gly)(H_2O)]$ and $[V^{IV}O(sal\text{-}Gly)(bipy)]$ with DNA are very similar above ca. 300 nm (Fig. S12), suggesting that with time complex **6** forms an adduct with DNA similar to that of $[V^{IV}O(sal\text{-}Gly)(H_2O)]$. Therefore, these observations indicate the existence of a new common species, which forms an adduct with DNA. As the band at ca. 370–380 nm significantly decreases its intensity, the process observed probably corresponds to the hydrolysis of the Schiff base, a distinct complex being involved in the binding to CT-DNA. One possibility is the formation of a $V^{IV}O$-salicylaldehyde complex.

For $[V^{IV}O(sal\text{-}Gly)(phen)]$ **7** the behavior of the UV–vis spectra with time differs from that of $[V^{IV}O(sal\text{-}Gly)(H_2O)]$ and $[V^{IV}O(sal\text{-}Gly)(bipy)]$; a small red shift (5 nm) in the band at 435 nm (to 440 nm) is observed as well as strong increase in the intraligand bands with maxima at 305 and 263 nm. All these bands show variations in its intensity, namely an increase in the 1st hour, followed by a decrease in the 2nd hour (for the intra-ligand bands, see Fig. S13). The final spectrum shows no resemblance with those obtained after 5 h with either **6** or $[V^{IV}O(sal\text{-}Gly)(H_2O)]$, suggesting a different interaction mechanism, which probably includes more than one binding type, one of which may be intercalation of the phenanthroline ligand between DNA bases.

3.3. DNA-binding study by CD spectroscopy

Circular dichroism (CD) is a spectroscopic technique widely used to study the affinity and binding modes of small molecules, such as metal compounds, to biomolecules, particularly DNA [66,67]. DNA is chiral due to being placed within the framework of the chiral sugar–phosphate backbone, producing a characteristic CD spectrum in the 200–300 nm range. Therefore, changes in the CD signal in this spectral range are useful to detect and follow DNA conformational changes, damage and/or cleavage [33,67–69]. Even when the complexes are achiral and thus present no CD signal, their association with the right-handed DNA helix may give rise to induced CD spectra (ICD) in the range where they have absorption bands.

CT-DNA shows a spectrum typical for right-handed B-form consisting of two bands: a positive one centered at 275 nm, due to base stacking;

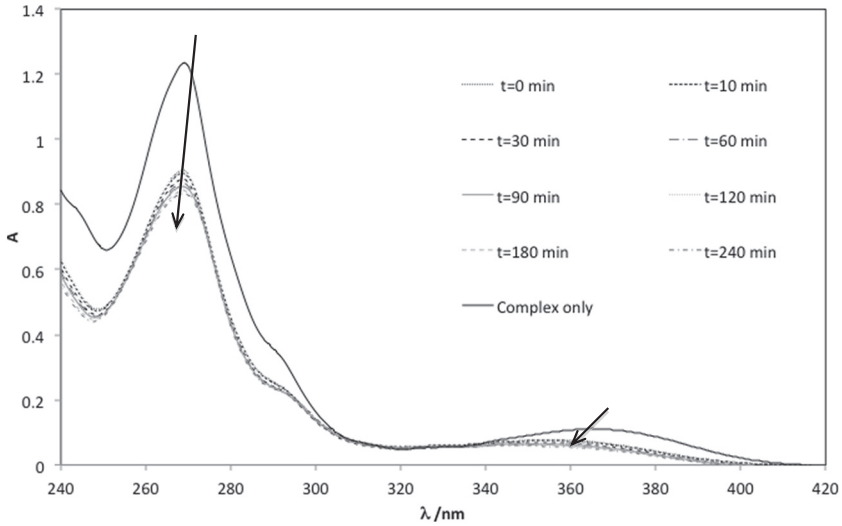

Fig. 2. UV–vis absorption spectra (2 mm optical path) of [Cu(sal-Gly)(phen)] (**2**) (100 μM) in the absence and presence of CT-DNA (400 μM) and changes observed with time. The arrows show the absorbance changes with increasing time.

Please cite this article as: I. Correia, et al., Vanadium(IV) and copper(II) complexes of salicylaldimines and aromatic heterocycles: Cytotoxicity, DNA binding and DNA cleavage pr..., J. Inorg. Biochem. (2015), http://dx.doi.org/10.1016/j.jinorgbio.2015.02.021

and a negative one at 245 nm due to right-handed helicity. It has been observed that intercalation leads to changes in intensities of both bands due to increased base stacking and helicity stabilization, while groove binding and electrostatic interactions result in small or no changes in the bands [70,71]. Additionally, intercalators generally exhibit small ICD signals (less than 10 M^{-1} cm^{-1}), with larger ICD signals being indicative of groove-binding interactions [66].

The conformational changes of CT-DNA induced by the complexes were monitored by CD spectroscopy. Upon mixing DNA with the non-chiral Cu^{II}-complexes, **1** and **2** (Figs. S14 and S15), changes are observed. For complex **1** the intensity of both bands slightly increase, but changes are more pronounced in the negative band associated to helicity. For complex **2**, changes are much more pronounced in the positive band associated with base stacking, which increases ca. 30%. These changes have been reported to correspond to partial DNA unwinding, as well as to induced circular dichroism of both, chiral and achiral, compounds upon their intercalation into DNA [66]. The large effect observed for **2** on the positive band suggests intercalation of the phentanthroline ligand between the DNA base pairs [70], possibly at the minor groove.

Fig. 3 shows the spectra measured for **3** in the absence and presence of CT-DNA (see also Fig. S17). Analysis of the CD data measured for the optically active complexes [Cu(sal-L-Ala)(phen)] **3** and [Cu(sal-D-Ala)(phen)] **4** is not straightforward since the CD spectra below 300 nm has contributions from both DNA and the metal complexes. However, the spectrum resulting from subtraction of the CD spectrum of the complex (**3** or **4**) from the experimental spectrum of (DNA + complex) (see Figs. S16 and S18) shows that, for both **3** and **4**, the intensity of the positive DNA band at 275 nm increases upon mixing with the Cu^{II}-complexes, similar to the effect observed with complex **2**. These results suggest that DNA is undergoing similar conformational changes upon interaction with **2**, **3** or **4** and that the phenanthroline ligand is intercalating DNA [70].

For [V^{IV}O(sal-Gly)(H_2O)] the CD spectra measured for solutions containing the complex and DNA depict small but significant perturbations in the negative band, which increases its intensity (Fig. S19), but no significant changes are detected in the positive CD band with λ_{max} at ~275 nm. The changes observed in the negative band resemble those observed for complex **1** (although less pronounced), indicating changes in the DNA conformation. For complex [V^{IV}O(sal-Gly)(bipy)] **6** similar spectral changes were observed. For [V^{IV}O(sal-Gly)(phen)] **7** the positive band is the most affected one as is shown in Fig. 4; the band shows a decrease in intensity as well as a bathochromic shift, an observation indicative of intercalation of the complex.

For the chiral vanadium complexes [V^{IV}O(sal-L-Phe)(bipy)] **9** and [V^{IV}O(sal-L-Phe)(phen)] **10** (see Figs. 5 and 6) the intensity of the d-d bands in the visible range decrease with time and isodichroic points are discernible (e.g. at 570 nm for **9**), suggesting the formation of a new species, probably an adduct between the complex and DNA [61]. Fig. 5 shows the spectra measured in the UV–vis range for complex **9** in the absence and presence of CT-DNA. Both the negative band at 371 nm and the positive at ca. 700 nm decrease in intensity upon mixing with DNA and with increasing time. Moreover, the band at 371 nm is blue shifted to 366 nm (at 150 min) and an isodichroic point appears at ca. 570 nm. These changes are consistent with the formation of a new species. The spectra measured in the UV range show that DNA is undergoing changes in both bands. The spectrum obtained after subtraction of the CD contribution from the chiral complex in this range evidences that the negative band increases and the positive band is red shifted (see Fig. S22).

For complex **10** the changes are more pronounced since there is a 55% decrease in the intensity of the negative band with maximum at 390 nm after 2.5 h, although most changes are observed within the 1st hour; a blue shift to 371 nm also occurs. Moreover, the intensity of all d-d bands decrease. In the UV range the corrected spectra (after subtraction of the complex spectrum) show changes that are more pronounced in the positive band.

All these observations are consistent with the (a) progressive oxidation of V^{IV} to V^{V}; (b) progressive decomposition of the Schiff base ligand (as the band at ca. 380–390 nm decrease intensity); (c) intercalation of the phenanthroline of the new V-species, which contains this co-ligand, between base pairs of the DNA helix [61]. Thus, for the vanadium complexes the CD data shows quite significant effects and changes with time for the complexes containing phenanthroline as co-ligand.

The progressive oxidation of V^{IV} to V^{V} was corroborated by ^{51}V-NMR: the possible formation of V(V)-complexes in a solution containing CT-DNA and [V^{IV}O(sal-Gly)(phen)] (600 and 150 μM, respectively), in contact with air at pH 7.4, was periodically checked by ^{51}V-NMR up to 24 h, showing the presence of a weak V^{V} peak at −556 ppm, which increased with time (see Fig. S27). This is the region where monovanadate resonates at pH 7.4 [72], confirming the partial hydrolysis and oxidation of the V^{IV}, resulting in the displacement of the ligands.

3.4. Fluorescence experiments

To gain further insight on the DNA binding properties of the complexes, fluorescence spectroscopy studies were carried out. Complex **2**

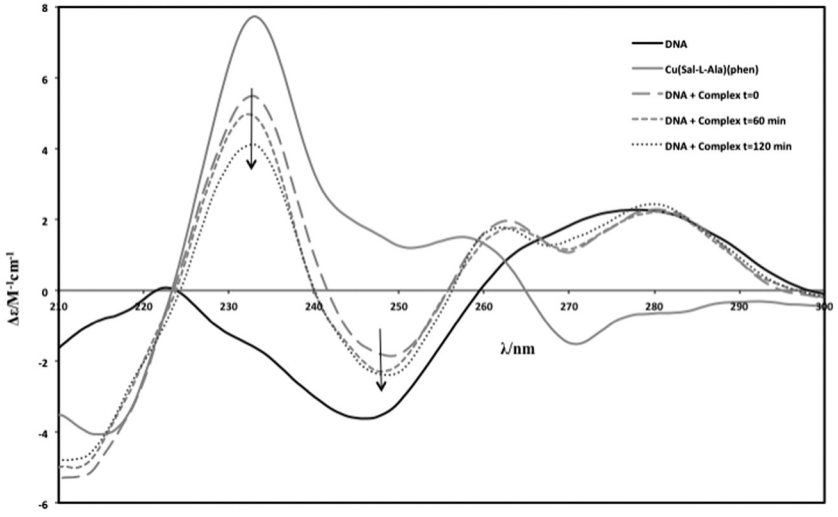

Fig. 3. Circular dichroism spectra (1 mm optical path) of CT-DNA (400 μM) in the absence and presence of [Cu(sal-L-Ala)(phen)] (**3**) (100 μM) in PBS buffer (pH 7.4). Arrows show the absorbance trend with time. The CD spectrum measured for the complex is also included for comparison.

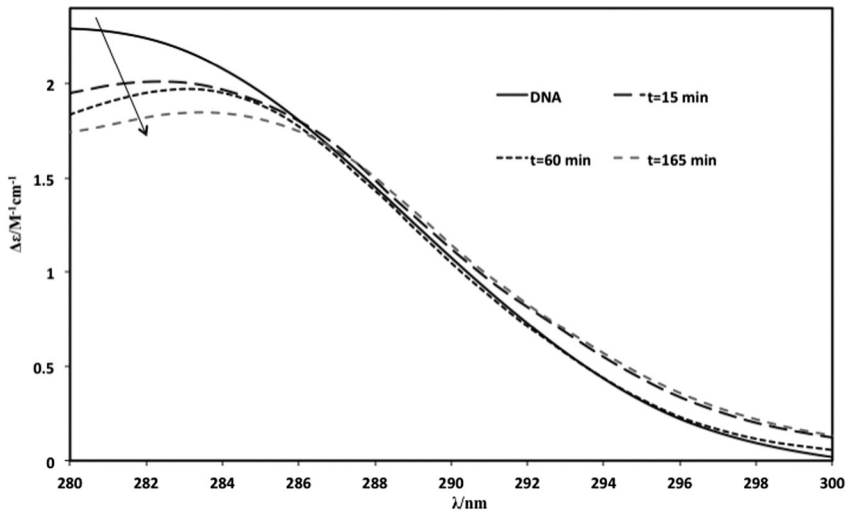

Fig. 4. Circular dichroism spectra, measured with a 10 mm optical path quartz cell, of CT-DNA (400 μM) in the absence and presence of [$V^{IV}O$(sal-Gly)(phen)] (**7**) (100 μM) in PBS buffer (pH 7.4). The arrow shows the absorbance trend with time.

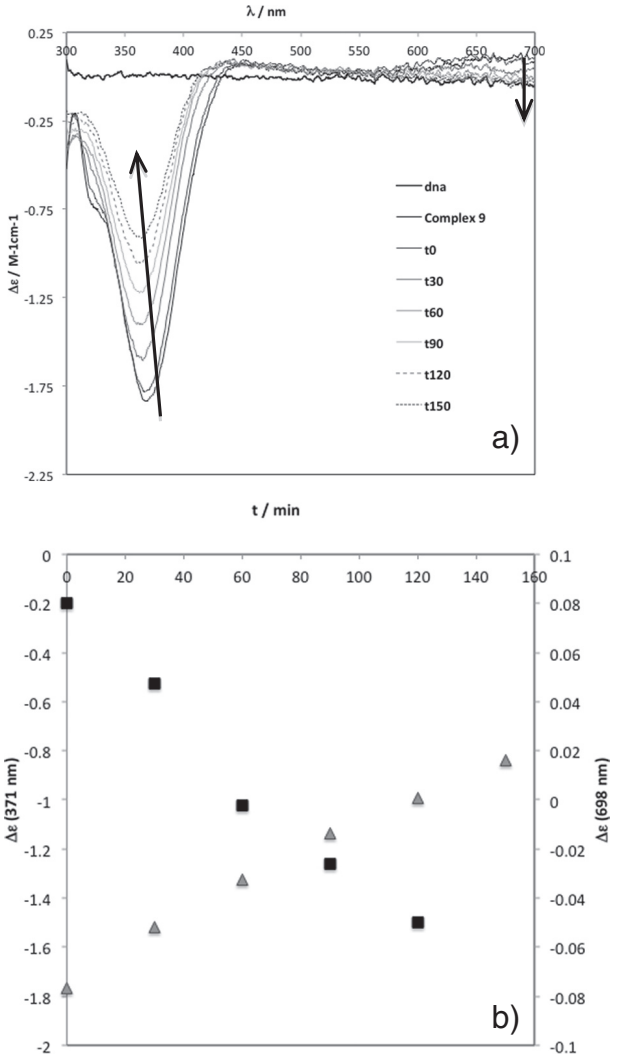

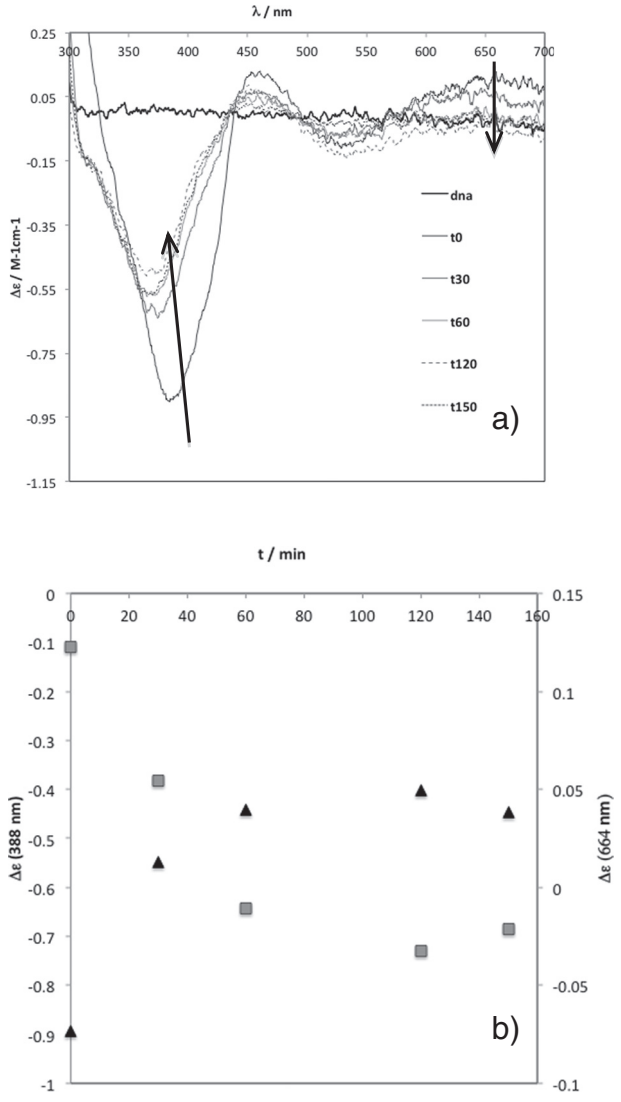

Fig. 5. (A) Circular dichroism spectra (10 mm optical path) measured with time for CT-DNA (400 μM) in the absence and presence of [VO(sal-L-Phe)(bipy)] (**9**) (100 μM) in PBS buffer (pH 7.4). The arrows show the absorbance changes with time. B) Variation of Δε at 371 (black squares) and 698 nm (gray triangles) with time.

Fig. 6. (A) Circular dichroism spectra (10 mm optical path) measured with time for CT-DNA (400 μM) in the absence and presence of [$V^{IV}O$(sal-L-Phe)(phen)] (**10**) (100 μM) in PBS buffer (pH 7.4). The arrows show the absorbance trend with time. B) Variation of Δε at 388 (black triangles) and 664 nm (gray squares) with time.

Please cite this article as: I. Correia, et al., Vanadium(IV) and copper(II) complexes of salicylaldimines and aromatic heterocycles: Cytotoxicity, DNA binding and DNA cleavage pr..., J. Inorg. Biochem. (2015), http://dx.doi.org/10.1016/j.jinorgbio.2015.02.021

shows fluorescence when exited at 360 nm and a titration with increasing amounts of DNA was carried out. Increasing fluorescence intensity (ca. 25%) was observed with increasing DNA concentration, and saturation was obtained for ca. [DNA]/[**2**] > 1.4, indicating that upon addition of DNA the complex is protected from quenching by the solvent molecules. The Stern–Volmer plot is linear up to [DNA]/[**2**] = 1.3 and the K_{SV} constant obtained was $1.83 \times 10^3\ M^{-1}$. These observations confirm that the complex is able to interact with DNA and that the process probably involves intercalation, since this binding process protects the complex from solvent quenching.

Competitive binding experiments based on the displacement of the intercalating drug ethidium bromide from CT-DNA were also done. If the complex displaces EB from DNA, the fluorescence of EB decreases due to free EB molecules being less fluorescent than the DNA bound EB molecules, because solvent molecules quench the fluorescence of free EB. However, not only the DNA intercalators but also groove DNA binders can cause the reduction in the emission intensities of DNA bound EB, but to a lower extent.

This study started with optimization of the ratio of [DNA] to [EB] by fixing the DNA concentration at 10 μM and varying the EB concentration. As expected, increasing fluorescence intensity was observed with increasing [EB] and saturation was obtained for ca. 10 μM of EB. Next, different amounts of complexes **2** or **5** were added to the saturated EB–DNA solution. The corresponding emission spectra, in the absence and in the presence of increasing amounts of each copper complex (**2** and **5**) are depicted in Fig. 7. Both complexes were able to reduce the fluorescence intensity (to 80–85%), indicating that they are able to compete with EB for the same binding sites, or interact with DNA at different sites. The Stern–Volmer plot obtained for complex **5** using the data collected for ratios of [**5**]/[DNA] < 2 is also shown in Fig. 7 and the K_{SV} obtained was $6.9 \times 10^3\ M^{-1}$. However, there are different binding modes, concentration dependent. The non-linearity of the Stern–Volmer plot, which shows an upward curvature (for complex **2**) is usually indicative of a combination of static and dynamic quenching processes.

Generally, the linearity of the Stern–Volmer plot has two meanings: the existence of one binding site for the ligand in the proximity of the fluorophore, or more than one binding site equally accessible to the ligand. Thus the gradual deviation from linearity of the Stern–Volmer plots on continuous addition of the complex is indicative of the existence of more than one binding site with different accessibilities and/or the occurrence of combined quenching. The Stern–Volmer plot of complex **2** (made only for the sake of comparison, see SI, K_{SV} (**2**) = $4.5 \times 10^3\ M^{-1}$) shows that the binding is stronger for complex **5** than for complex **2**, although they are of the same order (10^3). If intercalation of the phen ligand was the only binding mode responsible for the interaction, roughly the same value should have been obtained. In the present systems, although compound **5**, containing phenylalanine, corresponds to much higher steric hindrance upon intercalation, as compared with **2**, it also allows extra van der Waals interactions, and the DNA binding is stronger for **5**. These results correlate well with the cytotoxicity studies (see below) which show that in most cell types (except MCF7) complex **5** is more cytotoxic than **2**.

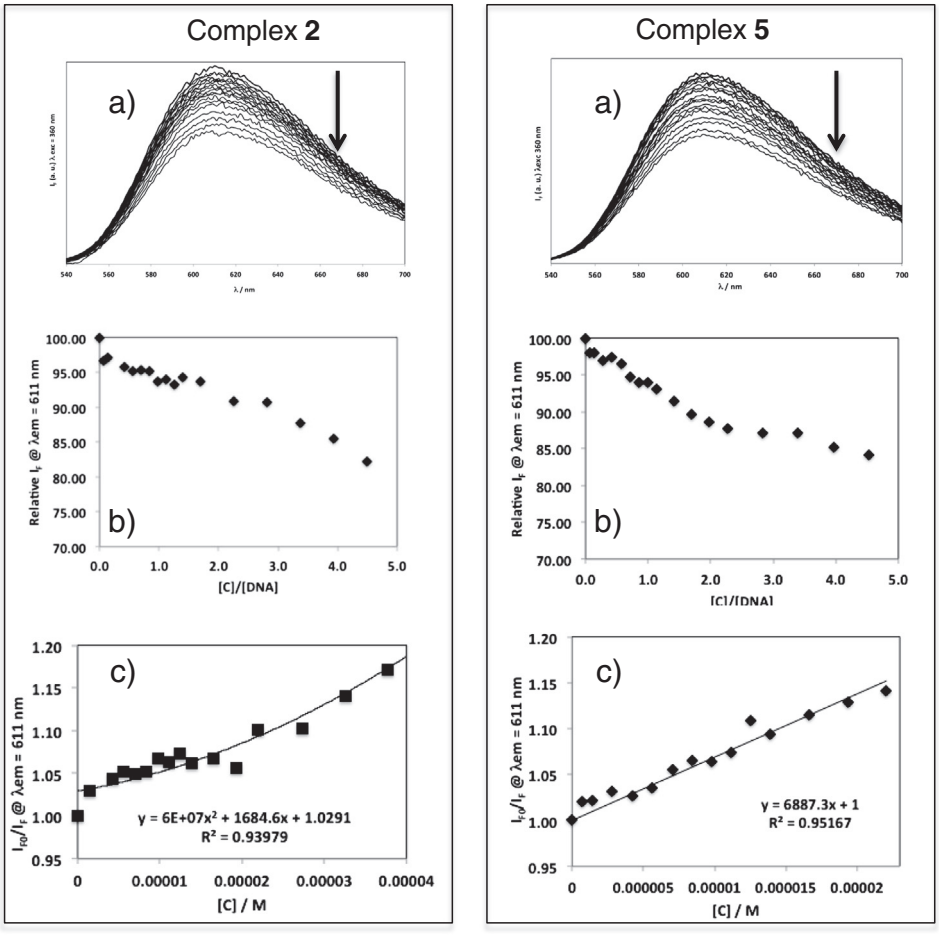

Fig. 7. Effect of complexes **2** and **5** in DNA–EB fluorescence. (a) Emission spectra (λ_{exc} = 360 nm) of the DNA–EB complex (10 μM:10 μM) in the absence and in the presence of increasing concentrations of **2** and **5** in 5% EtOH/PBS pH 7.4 (arrows indicate the variation observed with increasing concentration of complexes). b) Relative Fluorescence intensity (%) at λ_{em} = 611 nm with increasing complex concentration (ratios of [C]/[DNA] indicated). (c) Stern–Volmer plots at 611 nm obtained from steady-state (I_{F0}/I_F) measurements for each system (I_{F0}/I_F data was corrected for inner-filter-effects).

Please cite this article as: I. Correia, et al., Vanadium(IV) and copper(II) complexes of salicylaldimines and aromatic heterocycles: Cytotoxicity, DNA binding and DNA cleavage pr..., J. Inorg. Biochem. (2015), http://dx.doi.org/10.1016/j.jinorgbio.2015.02.021

3.5. DNA cleavage activity

To evaluate the nuclease ability of the complexes, DNA cleavage on plasmid DNA was monitored by agarose gel electrophoresis (AGE). The naturally occurring supercoiled form (Form I), when nicked, gives rise to an open circular relaxed form (Form II) and upon further cleavage, results in the linear form (Form III). When subjected to gel electrophoresis, faster migration is observed for Form I. The open circular Form II is slower, due to its less compact geometry, and Form III migrates between Forms I and II. The distribution of the three DNA forms in agarose gel electrophoresis provides a measure of the extent of DNA cleavage. We highlight that the DNA used in these experiments does not contain EDTA; this being a sequestering agent for many metal ions [7], the gel-electrophoretic results may be meaningless if it is present in DNA-cleavage studies during incubation of the samples.

The effect of Cu^{II}- (**1**, **2** and **5**) and $V^{IV}O$-complexes (**6**–**9**) on plasmid DNA was studied using different complex concentrations at 37 °C during 1 or 5 h incubation periods in phosphate buffer (pH 7.2). After 1 h and at 50 μM all complexes were unable to induce any significant DNA cleavage. An increase in complex concentration to 100 μM and incubation time to 5 h (Fig. 8) still shows no significant activity for most complexes, with the exceptions of [Cu(sal-Gly)(phen)] **2** and [Cu(sal-L-Phe)(phen)] **5**, which yield extensive single-stranded and also double-stranded DNA cleavage. Further experiments (Fig. 9) confirmed that the process is concentration dependant (see Fig. S24). Compounds **7**, **9** and **10** did not dissolve completely in the buffer medium used, which may be the reason for their inactivity.

Since redox agents are present at the cellular level and may activate Cu and V complexes to produce strand scission, further experiments were done in the presence of oxone as oxidizing agent and MPA (3-mercaptopropionic acid) as reducing agent. In the presence of oxone and after 5 h of digestion (Fig. 10) all complexes promote extensive DNA degradation. Samples of [Cu(sal-Gly)(bipy)] **1**, [Cu(sal-Gly)(phen)] **2** and [Cu(sal-L-Phe)(phen)] **5** with oxone show no bands, suggesting there was complete degradation of DNA into small strands undetectable by AGE. Vanadium complexes [$V^{IV}O$(sal-Gly)(phen)] **7** and [$V^{IV}O$(sal-L-Phe)(phen)] **10** completely decompose the Sc form into linear and nicked forms (Fig. 10a), while [$V^{IV}O$(sal-L-Phe)(bipy)] **9** does it only partially (Fig. 10a) and [$V^{IV}O$(sal-Gly)(bipy)] **6** is the least active one (Fig. 10b). Hence, activation by oxone results in the following order of nuclease activity: **1**, **2**, **5** > **7**, **10** > **9** > **6**.

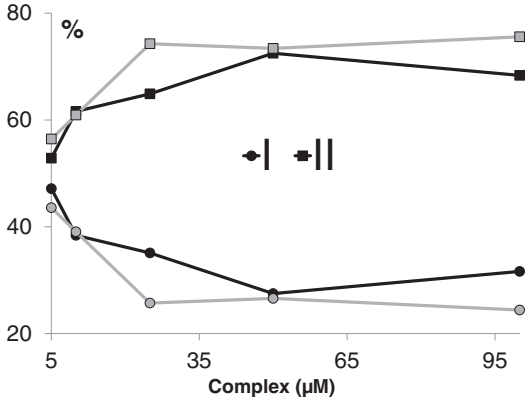

Fig. 9. Relative amounts of the Form I (Sc) and II (Nck) of DNA, measured after incubation, as function of the concentrations of **2** (black) and **5** (gray). The areas were measured by densitometry from the corresponding bands in the agarose gel image (Fig. S24) and are represented as percentage of each form.

It was previously reported that [73], among several vanadium complexes which show inhibition of cell growth for human nasopharyngeal carcinoma KB cells, $V^{IV}O(phen)^{2+}$ cleaved Col E1 plasmid DNA effectively in the presence of H_2O_2, $V^{IV}OSO_4$ being much less active. It was proposed that $V^{IV}O(phen)^{2+}$ binds DNA and that $^{\bullet}OH$ radicals were the active species in the cleavage process. In the present systems the efficacy of the several $V^{IV}O$-complexes changes with the nature of the sal-amino acidato ligand, and we do not expect that the active cleaving species might be $V^{IV}O(phen)^{2+}$ resulting from decomposition of the complexes. However, it is probable that the mechanism is oxidative and associated with the formation of ROS.

In the presence of MPA (Fig. 11) similar dramatic changes were not observed. However, in the reaction of **2** and **5** with plasmid DNA, the latter was extensively destroyed (Fig. 11a) as no bands are detected. Complexes **1**, **10** and **7** break double strand pDNA when MPA is added; complexes **9** (Fig. 11a) and **6** (Fig. 11b) promote single stranded cleavage. Thus, activation by MPA results in the following order of nuclease activity: **2**, **5** > **1** > **7**, **10** > **6**, **9**. It is expected that MPA will strongly activate Cu^{II}-complexes by reducing them to Cu^{I}, while $V^{IV}O$-complexes are unaffected. The formed Cu^{I}-species activates O_2, forming a hydroxyl

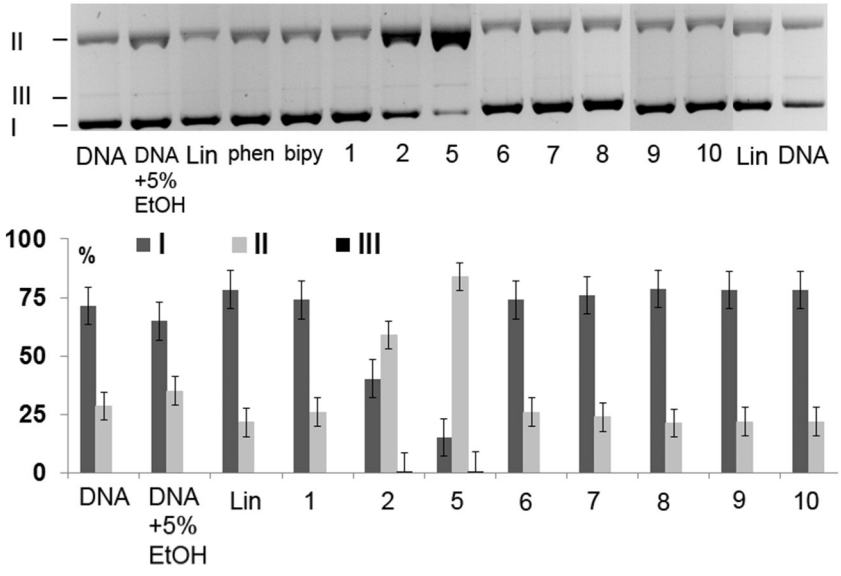

Fig. 8. DNA cleavage activity of compounds **1, 2, 5**–**10** (100 μM) in 10 mM PBS buffer, containing EtOH. "DNA" and "Lin" represent controls for the Sc and Lin forms of DNA. "DNA + 5% EtOH" is the control for the Sc DNA (in buffer solution containing 5% EtOH). "Phen" and "bipy" are controls for 1,10-phenanthroline and 2,2′-bipyridine. All samples were incubated for 5 h at 37 °C. Upper and lower parts are, respectively, the gel image and the bar chart showing the percentage of each DNA band; error bars represent S_r.

Please cite this article as: I. Correia, et al., Vanadium(IV) and copper(II) complexes of salicylaldimines and aromatic heterocycles: Cytotoxicity, DNA binding and DNA cleavage pr..., J. Inorg. Biochem. (2015), http://dx.doi.org/10.1016/j.jinorgbio.2015.02.021

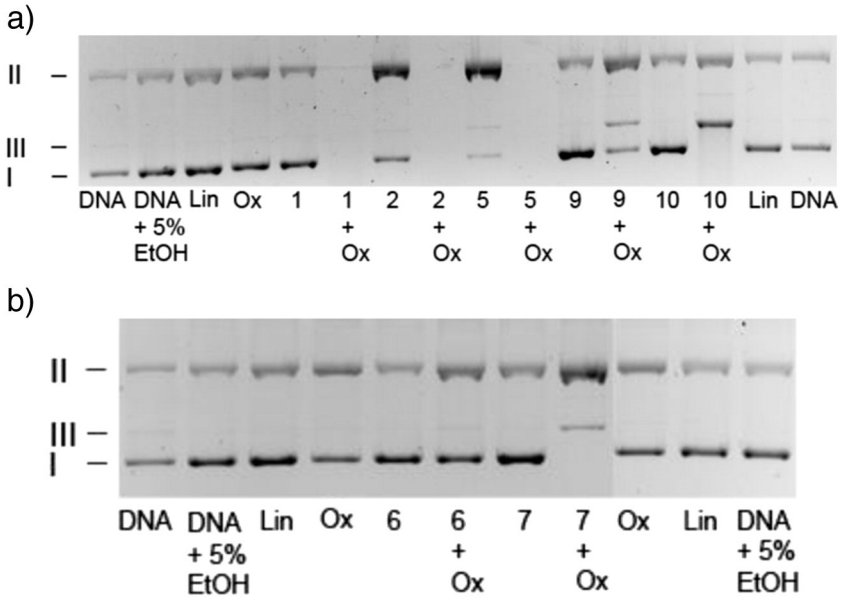

Fig. 10. Cleavage of pDNA by compounds **1**, **2**, **5**–**10** in the absence and presence of oxone. The complexes were dissolved in 20 mM PBS buffer containing 5% EtOH. "DNA" and "Lin" represent controls for Sc and Lin forms of DNA. "DNA + 5% EtOH" is the control for the Sc DNA in buffer containing 5% EtOH. "Ox" is the control for oxone without addition of any complex. a) Samples in lanes 1–14 were incubated for 5 h and those of lanes 15 and 16 for 2 h at 37 °C. b) Samples in lanes 1–8 were incubated for 5 h, those of lanes 3–15 for 2 h at 37 °C and those of lane 16 for 5 h at room temperature.

radical and/or Cu-oxo species which cleaves DNA by abstraction of the deoxyribose H atom [74]. The presence of phenantroline as ligand clearly increased this effect. Phenanthroline being a DNA intercalator, promotes a closer proximity of Cu to the sugar molecules, this increasing the probability of ROS attack, while the bipy containing complexes do not show such similar effects.

In general, at 50 μM most of the supercoiled DNA is converted to nicked form and a small percentage to linear form. At higher concentrations, the nuclease activity increased with supercoiled DNA converted to the linear form and the appearance of a smear, indicative of extensive DNA cleavage. For **1**, **2** and **5**, this effect is much stronger, leading to the detection of the DNA smear even at 50 μM. The presence of MPA/oxone has a significant effect, more remarkable for **2** and **5** where the linear form is observed in large extent.

Therefore, we conclude that all complexes show strong nuclease activity in the presence of activating agents, **2** and **5** being able to cleave DNA even in the absence of activating agents. Globally the Cu^{II} complexes are more active than the $V^{IV}O$-compounds and complexes **1**, **2** and **5** are the most efficient DNA cleavers within the compounds considered in this work.

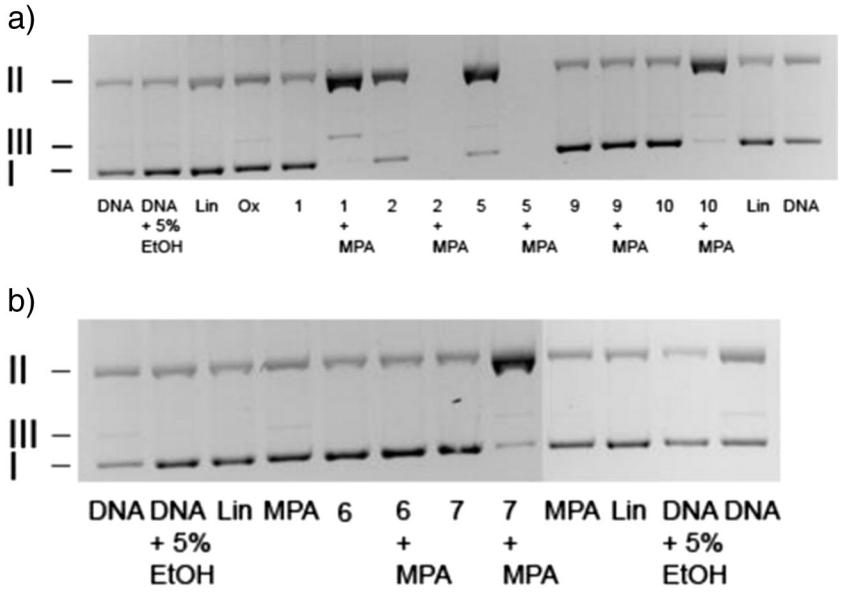

Fig. 11. Cleavage of pDNA by compounds **1**, **2**, **5**–**10** in the absence and presence of MPA. The complexes were dissolved in 20 mM PBS buffer containing 5% EtOH. "DNA" and "Lin" represent controls for Sc and Lin forms of DNA. "DNA + 5% EtOH" is the control for the Sc DNA in buffer containing EtOH. "MPA" is the control for MPA without addition of any complex. a) Samples in lanes 1–14 were incubated for 5 h and those of lanes 15 and 16 for 2 h at 37 °C. b) Samples in lanes 1–12 were incubated for 5 h, those of lanes 13–15 for 2 h at 37 °C and those of lanes 16 for 5 h at room temperature.

Please cite this article as: I. Correia, et al., Vanadium(IV) and copper(II) complexes of salicylaldimines and aromatic heterocycles: Cytotoxicity, DNA binding and DNA cleavage pr..., J. Inorg. Biochem. (2015), http://dx.doi.org/10.1016/j.jinorgbio.2015.02.021

These observations were further corroborated by AFM studies, which are included in SI (see Figs. S25 and S26). After 24 h of incubation of plasmid DNA with selected Cu^{II} and $V^{IV}O$-complexes at 37 °C, changes in the shape of plasmid DNA, such as supercoiling and kinks were observed. These effects appear more intense for the phen-containing complexes than for their bipy analogues, and complex **5** is the one that shows more changes for the same incubation time, however, the obtained images lack quality and further studies are required to allow a deeper understanding of these systems from AFM images.

3.6. Cytotoxicity studies

The cytotoxicity of complexes **1**–**10** was evaluated on human MCF7 breast and A2780 ovarian cancer cells. For comparative purposes, cisplatin was also included in the study. Fig. 12 shows the concentration response curves found for the Cu^{II}- and $V^{IV}O$-complexes, which was evaluated for an incubation period of 72 h with both types of cells. The IC_{50} values were measured using the colorimetric MTT assay and are presented in Table 1 as well as those determined for complexes **1, 2, 5** and cisplatin on HL60 (human promyelocytic leukemia cells) and HeLa (human cervical cancer cells).

In general, the measured IC_{50} values show that for MCF7 and A2780 cells, after 72 h of incubation, the Cu^{II}-compounds are more active than the $V^{IV}O$-complexes (except [Cu(sal-Gly)(bipy)]) and that the phen-containing complexes are more active than the corresponding bipy-containing ones. This is in agreement with the DNA cleavage studies that demonstrated the higher ability of the copper complexes to cleave plasmid DNA. Furthermore, the Cu^{II}-complexes containing phenanthroline are ca. 10-fold more cytotoxic than cisplatin.

The results of cytotoxicity against Hela and HL60 cell lines confirm the lower activity of [Cu(sal-Gly)(bipy)] when compared with the phen-containing compounds, especially [Cu(sal-L-Phe)(phen)], although their dynamics of action compared to cisplatin does not vary much between data taken at 24 and 72 h. This is also in line with the electrophoretic and spectroscopic studies.

Moreover, when comparing the activities of [Cu(sal-L-Ala)(phen)] and [Cu(sal-D-Ala)(phen)] it may be concluded that the chirality of the amino acid in the Schiff ligand does not affect the cytotoxic activity.

4. Conclusions

Oxidovanadium(IV) and copper(II) Schiff base complexes derived from salicylaldehyde and amino acids, containing H_2O, phen or bipy as co-ligands were prepared and characterized. When dissolved in aqueous buffer solutions at pH 7.4 the [M(sal-AA)(NN)] compounds are much more stable to hydrolysis (and also to oxidation in the case of $V^{IV}O$-complexes) than the corresponding [M(sal-AA)(H_2O)] complexes, the Cu^{II}-compounds being significantly more stable than the $V^{IV}O$ with the same ligands.

The binding affinity towards CT-DNA studies demonstrated that all complexes induce conformational changes in DNA, some forming adducts, others by groove binding and/or by intercalating phenantroline co-ligands between the DNA base pairs. Competition fluorescence studies done with ethidium bromide showed the higher DNA binding ability

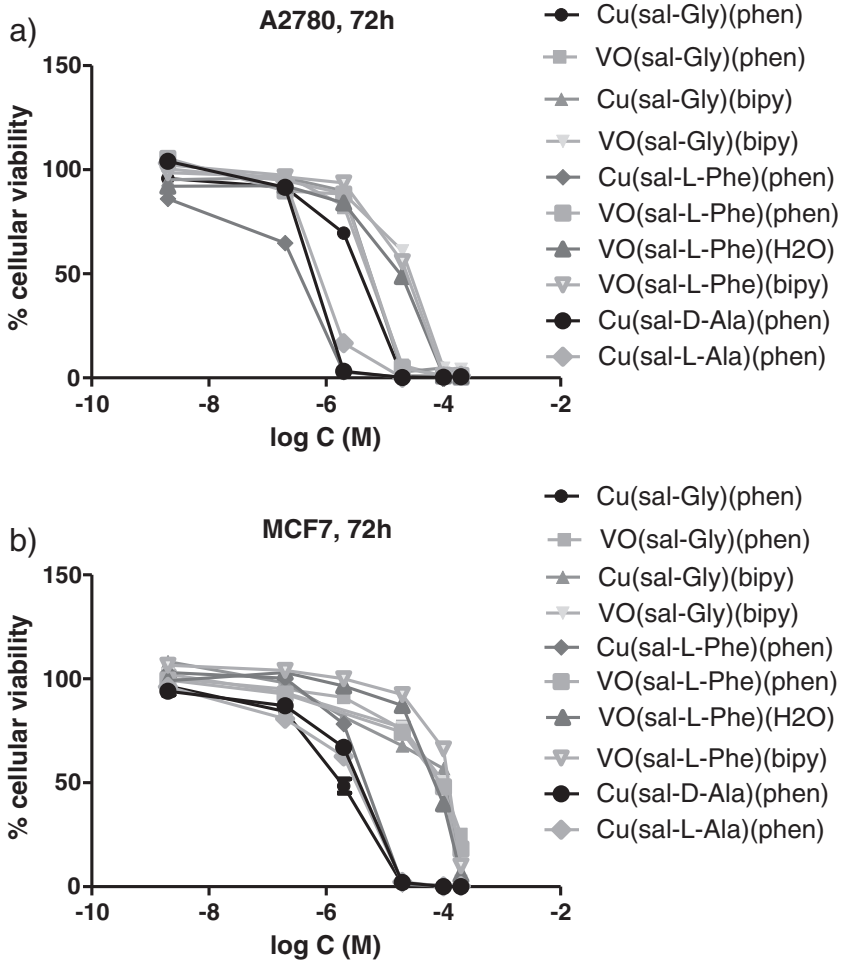

Fig. 12. Concentration–response curves obtained upon incubation of the (A) A2780 and (B) MCF7 cells for 72 h with the complexes indicated (see text for details).

Please cite this article as: I. Correia, et al., Vanadium(IV) and copper(II) complexes of salicylaldimines and aromatic heterocycles: Cytotoxicity, DNA binding and DNA cleavage pr..., J. Inorg. Biochem. (2015), http://dx.doi.org/10.1016/j.jinorgbio.2015.02.021

Table 1
IC_{50} (μM) determined for the metal complexes with different cancer cell lines.

	A2780	MCF7	HL-60		HeLa	
Compound	72 h	72 h	24 h	72 h	24 h	72 h
Cu(sal-Gly)(bipy) **1**	5.5 ± 1.9	52 ± 16	12.3 ± 7.6	12.6 ± 9.5	6.4 ± 24.4	14.4 ± 8.9
Cu(sal-Gly)(phen) **2**	3.2 ± 0.7	1.6 ± 0.3	6.3 ± 1.9	4.39 ± 1.43	7.1 ± 1.43	6.3 ± 2.0
Cu(sal-L-Ala)(phen) **3**	0.75 ± 0.2	2.5 ± 0.6				
Cu(sal-D-Ala)(phen) **4**	0.54 ± 0.2	2.7 ± 0.8				
Cu(sal-L-Phe)(phen) **5**	0.29 ± 0.01	3.5 ± 1.2	4.0 ± 1.3	1.51 ± 0.37	5.1 ± 1.4	4.2 ± 0.6
VO(sal-Gly)(bipy) **6**	20.8 ± 0.5	53 ± 20				
VO(sal-Gly)(phen) **7**	4.9 ± 1.3	77 ± 13				
VO(sal-L-Phe)(H_2O) **8**	14.1 ± 3.9	57 ± 16				
VO(sal-L-Phe)(bipy) **9**	17.1 ± 3.9	95 ± 37				
VO(sal-L-Phe)(phen) **10**	4.7 ± 1.8	68 ± 14				
Cisplatin	2.5 ± 0.1	28 ± 6.0	15.6 ± 1.2	2.2 + 0.1	20	4

of [Cu(sal-L-Phe)(phen)] **5** when compared to [Cu(sal-Gly)(phen)] **2**, and the co-existence of more than one type of binding mode.

The synthesized $V^{IV}O$-complexes do not exhibit significant nuclease activity in the absence of additives, but [Cu(sal-Gly)(phen)] **2** and [Cu(sal-L-Phe)(phen)] **5** are capable of double strand cleavage in rather harsh conditions, i.e. long (5 h) digestions and high complex concentration ($r_i = 6.7$), complex **5** being the most active. This was confirmed by AFM studies since complex **5** was the one that showed changes in collected plasmid DNA images. All complexes showed an enhanced nuclease activity in the presence of additives, namely of MPA or oxone. Cu^{II} complexes **2** and **5** are consistently the most active ones, while [V^{IV}O(sal-Gly)(bipy)] **6** is the most inert in all studied conditions.

Most of the complexes show cytotoxicity against different human tumor cell lines. The measured cytotoxicity and DNA cleavage ability show that [Cu(sal-L-Phe)(phen)] **5** is the most active. In general, the Cu^{II}-complexes showed much lower IC_{50} values (higher cytotoxic activity) than the corresponding vanadium complexes and the reference drug cisplatin (except [Cu(sal-Gly)(bipy)]). Moreover, the phenanthroline containing compounds are more cytotoxic than their bipyridine analogues. Globally, the cytotoxicity correlates well with the DNA cleavage activity, which showed the sequence **2, 5** > **1** > vanadium complexes; and with the DNA-binding ability determined for complexes **2** and **5** by fluorescence studies (**5** > **2**).

Acknowledgments

The authors thank the financial support from the Portuguese Fundação para a Ciência e Tecnologia, namely grants SFRH/BPD/74390/2010 and SFRH/BD/69444/2010, the program Investigador FCT and project UID/QUI/00100/2013. A.R. thanks the Spanish Ministry of Economía y Competitividad for the grant BES-2009-028024 associated to the project CTQ2008-02064. N.B. is grateful to the Erasmus Mundus External Cooperation Window-Lot 6 for the PhD grant.

Appendix A. Supplementary data

Supplementary data to this article can be found online at http://dx.doi.org/10.1016/j.jinorgbio.2015.02.021.

References

[1] B.K. Keppler, Metal Complexes in Cancer Chemotherapy, VCH, Weinheim and New York, 1993.
[2] J.C. Dabrowiak, Metals in Medicine, Wiley, 2009.
[3] D. Gambino, Coord. Chem. Rev. 255 (2011) 2193–2203.
[4] D. Crespy, K. Landfester, U.S. Schubert, A. Schiller, Chem. Commun. 46 (2010) 6651–6662.
[5] B. Gyurcsik, A. Czene, Future Med. Chem. 3 (2011) 1935–1966.
[6] F. Mancin, P. Scrimin, P. Tecilla, Chem. Commun. 48 (2012) 5545–5559.
[7] N. Butenko, A.I. Tomaz, O. Nouri, E. Escribano, V. Moreno, S. Gama, V. Ribeiro, J.P. Telo, J. Costa Pessoa, I. Cavaco, J. Inorg. Biochem. 103 (2009) 622–632.
[8] S. Gama, F. Mendes, F. Marques, I.C. Santos, M.F. Carvalho, I. Correia, J. Costa Pessoa, I. Santos, A. Paulo, J. Inorg. Biochem. 105 (2011) 637–644.
[9] S. Gama, I. Rodrigues, F. Marques, E. Palma, I. Correia, F.N.N. Carvalho, J. Costa Pessoa, A. Cruz, S. Mendo, I.C. Santos, F. Mendes, I. Santos, A. Paulo, RSC Adv. 4 (2014) 15.
[10] J.Z. Lu, H.W. Guo, X.D. Zeng, Y.L. Zhang, P. Zhao, J. Jiang, L.Q. Zang, J. Inorg. Biochem. 112 (2012) 39–48.
[11] A. Terenzi, M. Fanelli, G. Ambrosi, S. Amatori, V. Fusi, L. Giorgi, V.T. Liveri, G. Barone, Dalton Trans. 41 (2012) 4389–4395.
[12] J. Costa Pessoa, S. Etcheverry, D. Gambino, Coord. Chem. Rev. (2015)http://dx.doi.org/10.1016/j.ccr.2014.12.002 (in press).
[13] Y. Shechter, A. Shisheva, Endeavour 17 (1993) 27–31.
[14] K.H. Thompson, J.H. McNeill, C. Orvig, Chem. Rev. 99 (1999) 2561–2571.
[15] P. Caravan, L. Gelmini, N. Glover, F.G. Herring, H.L. Li, J.H. McNeill, S.J. Rettig, I.A. Setyawati, E. Shuter, Y. Sun, A.S. Tracey, V.G. Yuen, C. Orvig, J. Am. Chem. Soc. 117 (1995) 12759–12770.
[16] D. Rehder, J. Costa Pessoa, C.F.G.C. Geraldes, M.M.C.A. Castro, T. Kabanos, T. Kiss, B. Meier, G. Micera, L. Pettersson, M. Rangel, A. Salifoglou, I. Turel, D.G. Wang, J. Biol. Inorg. Chem. 7 (2002) 675–675.
[17] A.M. Evangelou, Crit. Rev. Oncol. Hematol. 42 (2002) 249–265.
[18] I. Kostova, Anticancer Agent Med. Chem. 9 (2009) 827–842.
[19] J. Benitez, L. Becco, I. Correia, S.M. Leal, H. Guiset, J. Costa Pessoa, J. Lorenzo, S. Tanco, P. Escobar, V. Moreno, B. Garat, D. Gambino, J. Inorg. Biochem. 105 (2011) 303–312.
[20] J. Benitez, L. Guggeri, I. Tomaz, J. Costa Pessoa, V. Moreno, J. Lorenzo, F.X. Aviles, B. Garat, D. Gambino, J. Inorg. Biochem. 103 (2009) 1386–1394.
[21] J. Benitez, A.C. de Queiroz, I. Correia, M.A. Alves, M.S. Alexandre-Moreira, E.J. Barreiro, L.M. Lima, J. Varela, M. Gonzalez, H. Cerecetto, V. Moreno, J. Costa Pessoa, D. Gambino, Eur. J. Med. Chem. 62 (2013) 20–27.
[22] M. Fernandez, L. Becco, I. Correia, J. Benitez, O.E. Piro, G.A. Echeverria, A. Medeiros, M. Comini, M.L. Lavaggi, M. Gonzalez, H. Cerecetto, V. Moreno, J. Costa Pessoa, B. Garat, D. Gambino, J. Inorg. Biochem. 127 (2013) 150–160.
[23] J. Benitez, I. Correia, L. Becco, M. Fernandez, B. Garat, H. Gallardo, G. Conte, M.L. Kuznetsov, A. Neves, V. Moreno, J. Costa Pessoa, D. Gambino, Z. Anorg. Allg. Chem. 639 (2013) 1417–1425.
[24] M. Fernandez, J. Varela, I. Correia, E. Birriel, J. Castiglioni, V. Moreno, J. Costa Pessoa, H. Cerecetto, M. Gonzalez, D. Gambino, Dalton Trans. 42 (2013) 11900–11911.
[25] D.C. Crans, J.J. Smee, E. Gaidamauskas, L.Q. Yang, Chem. Rev. 104 (2004) 849–902.
[26] D.C. Crans, M.L. Tarlton, C.C. McLauchlan, Eur. J. Inorg. Chem. (2014) 4450–4468.
[27] J. Costa Pessoa, E. Garriba, M.F.A. Santos, T. Santos-Silva, Coord. Chem. Rev. (2015) http://dx.doi.org/10.1016/j.ccr.2015.03.016 (in press).
[28] C.C. McLauchlan, B.J. Peters, G.R. Willsky, D. Crans, Coord. Chem. Rev. (2015) http://dx.doi.org/10.1016/j.ccr.2014.12.012 (in press).
[29] A. Bishayee, A. Waghray, M.A. Patel, M. Chatterjee, Cancer Lett. 294 (2010) 1–12.
[30] C. Duncan, A.R. White, Metallomics 4 (2012) 127–138.
[31] U. Jungwirth, C.R. Kowol, B.K. Keppler, C.G. Hartinger, W. Berger, P. Heffeter, Antioxid. Redox Signal. 15 (2011) 1085–1127.
[32] O. Zelenko, J. Gallagher, Y. Xu, D.S. Sigman, Inorg. Chem. 37 (1998) 2198–2204.
[33] S.C. Zhang, Y.G. Zhu, C. Tu, H.Y. Wei, Z. Yang, L.P. Lin, J. Ding, J.F. Zhang, Z.J. Guo, J. Inorg. Biochem. 98 (2004) 2099–2106.
[34] P.U. Maheswari, K. Lappalainen, M. Sfregola, S. Barends, P. Gamez, U. Turpeinen, I. Mutikainen, G.P. van Wezel, J. Reedijk, Dalton Trans. (2007) 3676–3683.
[35] P.U. Maheswari, S. Roy, H. den Dulk, S. Barends, G. van Wezel, B. Kozlevcar, P. Gamez, J. Reedijk, J. Am. Chem. Soc. 128 (2006) 710–711.
[36] L.J. Theriot, G.O. Carlisle, H.J. Hu, J. Inorg. Nucl. Chem. 31 (1969) 3.
[37] S. Mondal, S. Dutta, A. Chakravorty, J. Chem. Soc. Dalton Trans. (1995) 1115–1120.
[38] S. Dutta, S. Mondal, A. Chakravorty, Polyhedron 14 (1995) 1163–1168.
[39] I. Cavaco, J. Costa Pessoa, D. Costa, M.T. Duarte, R.D. Gillard, P. Matias, J. Chem. Soc. Dalton Trans. (1994) 149–157.
[40] Y. Nakao, K.I. Sakurai, A. Nakahara, Bull. Chem. Soc. Jpn. 40 (1967) 3.
[41] I. Cavaco, J. Costa Pessoa, M.T. Duarte, R.T. Henriques, P.M. Matias, R.D. Gillard, J. Chem. Soc. Dalton Trans. (1996) 1989–1996.
[42] J. Costa Pessoa, I. Cavaco, I. Correia, M.T. Duarte, R.D. Gillard, R.T. Henriques, F.J. Higes, C. Madeira, I. Tomaz, Inorg. Chim. Acta 293 (1999) 1–11.
[43] J. Costa Pessoa, M.J. Calhorda, I. Cavaco, I. Correia, M.T. Duarte, V. Felix, R.T. Henriques, M.F.M. Piedade, I. Tomaz, J. Chem. Soc. Dalton Trans. (2002) 4407–4415.

Please cite this article as: I. Correia, et al., Vanadium(IV) and copper(II) complexes of salicylaldimines and aromatic heterocycles: Cytotoxicity, DNA binding and DNA cleavage pr..., J. Inorg. Biochem. (2015), http://dx.doi.org/10.1016/j.jinorgbio.2015.02.021

[44] J. Costa Pessoa, M.J. Calhorda, I. Cavaco, P.J. Costa, I. Correia, D. Costa, L.F. Vilas-Boas, V. Felix, R.D. Gillard, R.T. Henriques, R. Wiggins, Dalton Trans. (2004) 2855–2866.
[45] I. Cavaco, J.C. Pessoa, M.T. Duarte, R.D. Gillard, P. Matias, Chem. Commun. (1996) 1365–1366.
[46] A.R. Chakravarty, J. Chem. Sci. 118 (2006) 443–453.
[47] P.A.N. Reddy, M. Nethaji, A.R. Chakravarty, Eur. J. Inorg. Chem. (2004) 1440–1446.
[48] P.A.N. Reddy, M. Nethaji, A.R. Chakravarty, Inorg. Chim. Acta 337 (2002) 450–458.
[49] P.K. Sasmal, A.K. Patra, M. Nethaji, A.R. Chakravarty, Inorg. Chem. 46 (2007) 11112–11121.
[50] U. Saha, T.K. Si, P.K. Nandi, K.K. Mukherjea, Inorg. Chem. Commun. 38 (2013) 43–46.
[51] A. Coutinho, M. Prieto, J. Chem. Educ. 70 (1993) 425–428.
[52] B. Valeur, Molecular Fluorescence. Principles and Applications, Wiley, Weinheim, 2001.
[53] M.B. Fisher, S.J. Thompson, V. Ribeiro, M.C. Lechner, A.E. Rettie, Arch. Biochem. Biophys. 356 (1998) 63–70.
[54] S. Nigam, Validation of methods for measuring efficiency of inorganic nucleases(MSc thesis) Universidade do Algarve, 2011.
[55] J. Bernadou, G. Pratviel, F. Bennis, M. Girardet, B. Meunier, Biochemistry-Us 28 (1989) 7268–7275.
[56] K. Nakamoto, Infrared and Raman Spectra of Inorganic Compounds, 5th ed. Wiley, 1997.
[57] J.M. Kelly, A.B. Tossi, D.J. Mcconnell, C. Ohuigin, Nucleic Acids Res. 13 (1985) 6017–6034.
[58] K.E. Erkkila, D.T. Odom, J.K. Barton, Chem. Rev. 99 (1999) 2777–2795.
[59] A.M. Pyle, J.P. Rehmann, R. Meshoyrer, C.V. Kumar, N.J. Turro, J.K. Barton, J. Am. Chem. Soc. 111 (1989) 3051–3058.
[60] H. Chao, W.J. Mei, Q.W. Huang, L.N. Ji, J. Inorg. Biochem. 92 (2002) 165–170.
[61] R.F. Pasternack, E.J. Gibbs, J.J. Villafranca, Biochemistry-Us 22 (1983) 2406–2414.
[62] E.C. Long, J.K. Barton, Acc. Chem. Res. 23 (1990) 271–273.
[63] L.P. Lu, M.L. Zhu, P. Yang, J. Inorg. Biochem. 95 (2003) 31–36.
[64] G.S. Son, J.A. Yeo, M.S. Kim, S.K. Kim, A. Holmen, B. Akerman, B. Norden, J. Am. Chem. Soc. 120 (1998) 6451–6457.
[65] G. Pratviel, J. Bernadou, B. Meunier, Adv. Inorg. Chem. 45 (1998) 251–312.
[66] N.C. Garbett, P.A. Ragazzon, J.B. Chaires, Nat. Protoc. 2 (2007) 3166–3172.
[67] J. Costa Pessoa, I. Correia, G. Gonçalves, A.I. Tomaz, J. Argent. Chem. Soc. 97 (2009) 151–165.
[68] A. Habib, M. Tabata, J. Inorg. Biochem. 98 (2004) 1696–1702.
[69] R.F. Vitor, I. Correia, M. Videira, F. Marques, A. Paulo, J. Costa Pessoa, G. Viola, G.G. Martins, I. Santos, Chem. Biol. Chem. 9 (2008) 131–142.
[70] L.M. Chen, J. Liu, J.C. Chen, S. Shi, C.P. Tan, K.C. Zheng, L.N. Ji, J. Mol. Struct. 881 (2008) 156–166.
[71] Z.F. Chen, X.Y. Wang, Y.Z. Li, Z.J. Guo, Inorg. Chem. Commun. 11 (2008) 1392–1396.
[72] L. Pettersson, I. Andersson, A. Gorzsas, Coord. Chem. Rev. 237 (2003) 77–87.
[73] H. Sakurai, H. Tamura, K. Okatani, Biochem. Biophys. Res. Commun. 206 (1995) 133–137.
[74] D.S. Sigman, T.W. Bruice, A. Mazumder, C.L. Sutton, Acc. Chem. Res. 26 (1993) 98–104.

Please cite this article as: I. Correia, et al., Vanadium(IV) and copper(II) complexes of salicylaldimines and aromatic heterocycles: Cytotoxicity, DNA binding and DNA cleavage pr..., J. Inorg. Biochem. (2015), http://dx.doi.org/10.1016/j.jinorgbio.2015.02.021